APPLIED PHYSICS LETTERS **89**, 172906 (2006)

Oxygen vacancy motion in Er-doped barium strontium titanate thin films

Junling Wang[a] and Susan Trolier-McKinstry[b]
Materials Research Institute, The Pennsylvania State University, University Park, Pennsylvania 16802

(Received 8 June 2006; accepted 7 September 2006; published online 25 October 2006)

Amphoteric dopants are widely used in $BaTiO_3$-based dielectrics to improve capacitor reliability. In this work, an analogous approach was explored for barium strontium titanate thin films. $Ba_{0.7}Sr_{0.3}TiO_3$ thin films were prepared by chemical solution deposition. Er was used as a dopant to decrease the leakage current and improve the film lifetime under dc electric field. The (Ba+Sr)/Ti ratio in the precursor solution was modified to facilitate doping on the *A* site, the *B* site, or both the *A* and *B* sites. It was observed that when (Ba+Sr)/Ti=1, the dopant has little effect on the dielectric constant, but decreases both the loss tangent and the leakage current. A current transient (peak) was observed prior to resistance degradation in both the undoped and Er-doped samples and was related to oxygen migration under dc bias. It is shown that Er doping effectively decreases the oxygen vacancy mobility, which may lead to longer lifetime under dc field in thin film $Ba_{0.7}Sr_{0.3}TiO_3$ capacitors. © *2006 American Institute of Physics*. [DOI: 10.1063/1.2364127]

High permittivity dielectric thin films have been studied extensively for applications in integrated capacitors, high-*k* insulators in dynamic random access memory, and tunable microwave devices.[1,2] These tunable elements rely on the field-dependent changes in the dielectric constant to perform their tasks and consequently experience high dc electric fields. One serious failure mechanism for perovskite-structured dielectrics exposed to high dc fields for long times is resistance degradation. In bulk ceramics, oxygen vacancies play a key role in resistance degradation.[3] It has been demonstrated that $BaTiO_3$ doped with Y, Ho, or Dy exhibits a combination of superior long-term reliability and tolerance to firing in reducing conditions.[4–6] The dopants utilized in $BaTiO_3$ are amphoteric ones that can sit on both the *A* and the *B* sites of the crystallographic lattice.[7] Rare earth doping of this type is now widely utilized in Ni-electroded bulk ceramic capacitors to increase their lifetime under applied dc field.[8–10] Despite the rich literatures on bulk $BaTiO_3$ capacitors, there have been few attempts to transfer this approach to the compositional engineering of thin films.[11–14] It is thus very interesting to explore amphoteric doping in thin films. If reliability improvements comparable to those in bulk dielectrics are achieved, it should be useful for thin film capacitors and integrated passive components.

The effective size of the *A* site ion decreases from a radius of 1.61 Å in $BaTiO_3$ to 1.559 Å in $Ba_{0.7}Sr_{0.3}TiO_3$, changing the unit cell volume from ~64.11 to ~62.3Å^3 at room temperature. As a result, it is possible that the optimum ion size for an amphoteric dopant to increase reliability in barium strontium titanate (BST) is smaller than that for $BaTiO_3$. Er^{3+} in 9 coordination has a radius of 1.062 Å, slightly smaller than Y^{3+}, Ho^{3+}, or Dy^{3+} (1.075–1.083 Å). The ratio of the volume of the Er^{3+} ion to the unit cell volume of $Ba_{0.7}Sr_{0.3}TiO_3$ is nearly identical to that of the volume of Y^{3+} relative to the volume of $BaTiO_3$, so it was hypothesized that Er^{3+} would be an ideal amphoteric dopant in $Ba_{0.7}Sr_{0.3}TiO_3$. Consequently, the focus of this work is to study the effect of Er doping on the dielectric and leakage properties of $Ba_{0.7}Sr_{0.3}TiO_3$ thin films, with a goal of understanding the effect of rare earth doping on oxygen vacancy motion under dc field.

Undoped and Er-doped thin films were prepared on $Pt/TiO_2/SiO_2/Si(100)$ substrates by chemical solution deposition. The precursor solutions were adapted from the work of Maria.[15] The (Ba+Sr)/Ti ratio was modified to facilitate Er doping on the *A* site, the *B* site, or both the *A* and *B* sites. Stoichiometric amounts of barium acetate, strontium acetate (with a molar ratio of 7:3), and erbium acetate were dissolved in glacial acetic acid and mixed at 110 °C for 1 h under an Ar atmosphere. Titanium isopropoxide was mixed with acetyl acetone, added into the solution, and refluxed for 1 h at 110 °C. Finally, 2-methoxyethanol was added to adjust the solution concentration to 0.1*M*.

The films were deposited by spinning the diluted solution at 3000 rpm for 30 s onto the substrate. Each layer (~17 nm) was dried at 170 °C for 3 min and then pyrolyzed at 375 °C for 3 min on a hot plate, followed by rapid thermal annealing at 710 °C in air for 2 min. This procedure was repeated until the desired thickness, typically 100–300 nm, was achieved. No significant thickness dependence of dielectric properties was observed within this range. The crystallinity of the films was characterized with a Scintag DMC-105 x-ray diffractometer using Cu $K\alpha$ radiation. The frequency and dc field-dependent dielectric characteristics were measured with an HP 4284A precision *LCR* meter. The leakage currents of the samples were measured with an HP4140B picoampere meter at temperatures up to 300 °C. Pt top electrodes of ~360 nm thick with area of $\sim 5.0 \times 10^{-4}$ cm^2 were deposited by sputtering through a shadow mask. Postdeposition annealing in air at 630 °C for 2 min was performed to improve the quality of the top electrode/film interface.

A set of ~130 nm thick films were prepared from precursor solutions batched with the compositions (a) $(Ba_{0.7}Sr_{0.3})TiO_3$, (b) $(Ba_{0.7}Sr_{0.3})Ti_{0.98}Er_{0.02}O_3$, (c) $(Ba_{0.7}Sr_{0.3})_{0.99}Ti_{0.99}Er_{0.02}O_3$, and (d) $(Ba_{0.7}Sr_{0.3})_{0.98}Er_{0.02}TiO_3$. X-ray diffraction showed no indication of second

[a]Present address: School of Materials Science and Engineering, Nanyang Technological University, Singapore 639798; electronic mail: jlwang@ntu.edu.sg
[b]Author to whom correspondence should be addressed; electronic mail: stmckinstry@psu.edu

© 2006 American Institute of Physics
Downloaded 19 Jun 2011 to 155.69.4.4. Redistribution subject to AIP license or copyright; see http://apl.aip.org/about/rights_and_permissions

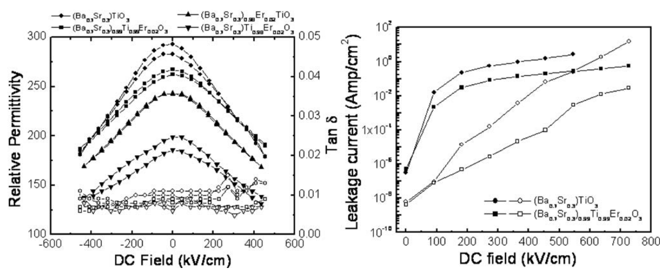

FIG. 1. (a) Electric field dependence of the dielectric constant (filled symbols) and loss (open symbols) of the *A* site, *B* site, and *A*/*B* site doped BST films (b) *I*-*V* characteristics of undoped and 2% Er-doped BST samples taken at room temperature (open symbols) and 200 °C (solid symbols) with a holding time of 100 s.

phases in any of them within detection limits. No significant difference in the lattice parameters was observed among the three samples within the resolution of our system. However, the dielectric properties of these films are clearly different, as shown in Fig. 1(a). The $(Ba_{0.7}Sr_{0.3})_{0.99}Ti_{0.99}Er_{0.02}O_3$ (*A*/*B* doped), where the Er dopant is expected to occupy both the *A* and *B* sites, has dielectric constant and loss values close to those of the undoped sample. The dielectric constants of these two samples are ~260 and 290 at 10 kHz under zero bias. A loss value as low as ~1% was observed. The *A*/*B* doped sample shows a slightly lower tunability. On the other hand, both $(Ba_{0.7}Sr_{0.3})_{0.98}Er_{0.02}TiO_3$ and $(Ba_{0.7}Sr_{0.3})Ti_{0.98}Er_{0.02}O_3$ films, where the Er dopant is expected to occupy predominantly the *A* or *B* site, respectively (driven by chemistry), show clear degradation in the dielectric constant, the tunability, and the dielectric loss. Films with Er on the *B* site show much lower dielectric constants and higher loss compared to samples where Er is expected to occupy the *A* site.

Leakage current measurements were carried out by applying negative voltage to the bottom electrode to minimize potential variability introduced with variations in the top electrode/film interface quality. By applying negative bias to the bottom electrode, electrons are injected into the film through the bottom interface, which varies little from sample to sample. The voltage was applied in a single step. A fresh capacitor was used for each voltage and temperature measurement. Given the degraded dielectric properties of films in which the Er was batched to occupy only the *A* or *B* site, the leakage study focused on the undoped and *A*/*B* doped samples.

It is observed through charging and discharging measurements that the polarization relaxation process completes after about 100 s in these samples. For long holding times, an increase in the leakage current develops. As discussed later in this letter, this is identified to be the front part of a current peak which may be associated with the motion of oxygen vacancies. After choosing the holding time (100 s) for the leakage measurement, current-voltage curves were measured at room temperature (open) and 200 °C (solid), as shown in Fig. 1(b). It is clear that the *A*/*B* doped BST film shows almost one order of magnitude smaller leakage currents at higher fields.

At elevated temperature, the leakage current versus time curve shows a peak, then falls prior to the onset of dielectric degradation. The time at which the peak is observed decreases with increasing applied field or temperature. Given that the electron/hole mobility is around 1 $cm^2/V\,s$,[16] the time required to develop the peak (seconds) is many orders of magnitude longer than would be characteristic of electron/hole transport across the film thickness. Consequently, the current peak is attributed to changes induced by oxygen vacancy redistribution, since oxygen vacancies are known to be mobile in titanate perovskites at these temperatures.[3]

Figure 2 shows the time dependent leakage current behavior for undoped and *A*/*B* doped samples measured at 200 °C under different dc fields. It is observed that the *A*/*B* doped (2% Er) sample shows lower leakage at all fields. In addition, the time required to develop the peak in the leakage is delayed in the *A*/*B* doped sample. Furthermore, the onset of dielectric degradation, which develops after the peak, is delayed in the *A*/*B* doped sample as well. These observations clearly indicate that the mobility of the oxygen vacancies is reduced in the *A*/*B* doped sample relative to undoped films.

The existence of a peak in the leakage data has been reported in the literature. Postulated explanations include a space-charge-limited-current transient, where the movement of charged oxygen vacancies contributes to the leakage current directly, causing the peak,[17,18] and modulation of the electron/hole conductivity due to oxygen vacancy redistribution.[3,19] For space-charge-limited-current transients, the time at which the current peak is observed is related to the drift mobility of the charge (oxygen vacancies in this case) by $\tau=0.78d^2/(\mu V)$, where τ is the time corresponding to the current peak, d is the film thickness, μ is the charge mobility, and V is the applied voltage. According to the theory,[20] a current transient peak would be observed upon the application of a voltage step only if a large reservoir of charge was available at the injecting electrode, which is not expected in our films. Furthermore, a very large concentration of oxygen vacancies would be needed for the current to be dominated by vacancy movement due to their substantially lower mobility (~10^{-8} $cm^2/V\,s$ at 200 °C) relative to electronic carriers.

Alternatively, Waser *et al.*[3] demonstrated that oxygen vacancy redistribution under dc fields can cause changes in the electron and hole conduction. In particular, Meyer *et al.* reported simulation results that reproduced the observed peak

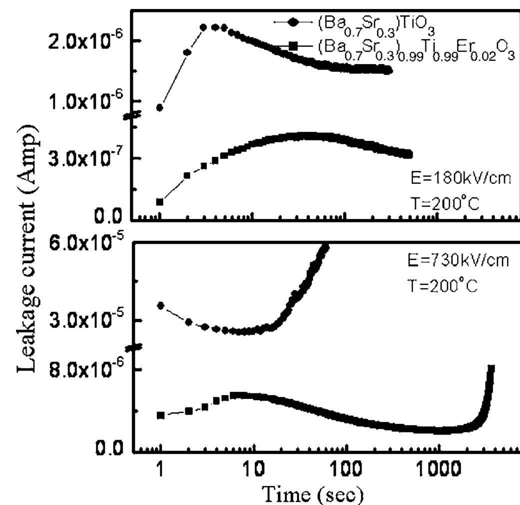

FIG. 2. Leakage current vs time behavior of undoped and 2% Er-doped BST samples measured at 200 °C under different fields. A delay in the current transient peak position is observed for the doped sample; likewise the onset of dielectric degradation was delayed.

Downloaded 19 Jun 2011 to 155.69.4.4. Redistribution subject to AIP license or copyright; see http://apl.aip.org/about/rights_and_permissions

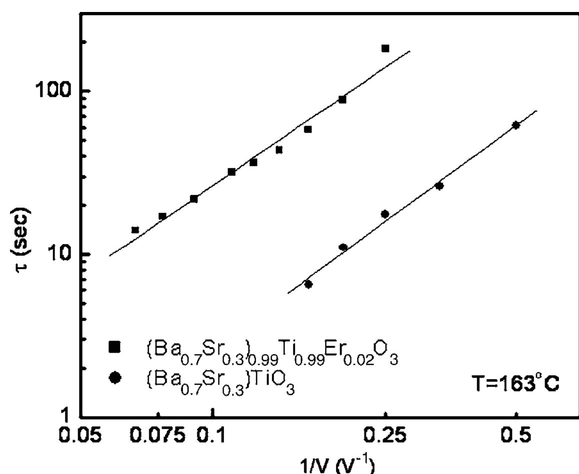

FIG. 3. Leakage current peak position at a function of $1/V$ plotted on log scale.

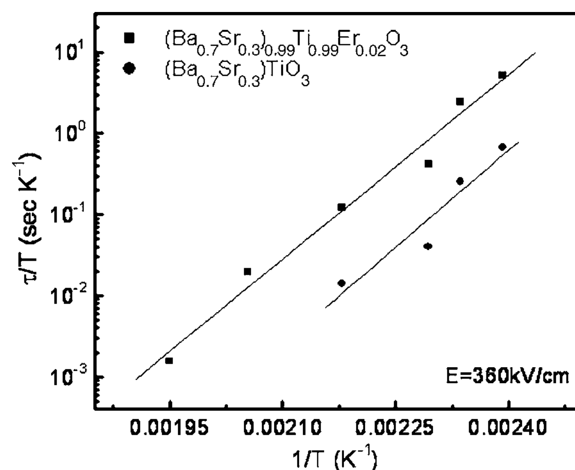

FIG. 4. Leakage current peak position as a function of $1/T$ measured at ~360 kV/cm.

in leakage current.[19] Following this approach, we attempt to extract the voltage acceleration factor and mobility of oxygen vacancies in the undoped and Er-doped $(Ba_{0.7}Sr_{0.3})TiO_3$ films. The critical time τ_{ch} is defined as the time when the current peak develops. Note that τ_{ch} was defined as the time when the leakage current has increased by one order of magnitude in Ref. 3. Empirically, $\tau_{ch} \propto d^{n_2}/(\mu V^{n_1})$ where V is the applied dc electric field, d is the thickness of the film, and μ is the mobility of oxygen vacancies. Thus, $\ln \tau_{ch} \propto n_1 \ln(1/V) + n_2 \ln d + \ln(1/\mu)$. Figure 3 shows the voltage dependence of τ_{ch} for films measured at 163 °C. Both doped and undoped films are well fitted by the above equation, where $n_1 \sim 1.96 \pm 0.11$ for $(Ba_{0.7}Sr_{0.3})TiO_3$ and $\sim 1.84 \pm 0.11$ for the Er-doped samples. These values are close to those obtained by Waser *et al.* Furthermore, the y axis intercepts in Fig. 3 give a qualitative comparison of the oxygen vacancy mobilities in the doped and undoped samples. It is observed that μ is smaller in the Er doped sample. It is possible that the Er dopants act as pinning centers for the oxygen vacancies through electrostatic or elastic interactions that slow down their movement.

The temperature dependence of τ_{ch}, as shown in Fig. 4, follows Arrhenius-type behavior. This is ultimately due to the oxygen vacancy diffusion activation energy, since τ_{ch} is inversely proportional to the oxygen vacancy mobility μ, and μ is related to the diffusion coefficient D through the Nernst-Einstein relation $\mu kT = qD$. Since $D = \gamma \exp(-E_0/kT), \tau/T \propto \exp(E_0/kT)$, where q is the ion charge, E_0 is the activation energy, k is Boltzmann's constant, and T is the temperature. Evaluating the data yields activation energies of $\sim 0.65 \pm 0.04$ and 0.69 ± 0.15 eV for the undoped and Er-doped $(Ba_{0.7}Sr_{0.3})TiO_3$, respectively. These values are smaller than those reported for $SrTiO_3$ and $BaTiO_3$ ceramics.[21,22] Please note that the critical time τ_{ch} in this letter is defined as the time when the current peak develops. In previous reports, e.g., Refs. 3 and 21, it was defined as the time when the leakage current increased by one order of magnitude, which happens after the current peak and leads to dielectric degradation. This suggests that the mechanisms responsible for the current peak and dielectric degradation may not be exactly the same. Further study is necessary to clarify this issue.

To conclude, Er-doped $(Ba_{0.7}Sr_{0.3})TiO_3$ films were prepared. Compared with both undoped films and with samples where the Er should be accommodated on predominantly the *A* or the *B* sites only, Er doping on both the *A* and *B* sites decreases the film leakage current while maintaining good dielectric properties. A peak was observed in the leakage current versus time characteristic, which is believed to relate to the motion of oxygen vacancies. It is shown that the Er doping effectively decreases the mobility of oxygen vacancies and thus may lead to longer lifetimes under applied bias fields. This suggests that amphoteric doping can be employed to improve the reliability of thin film perovskite titanate dielectrics, in the same manner as for bulk capacitors.

The authors gratefully appreciate the financial support of Intel, Inc.

[1] *Nanoelectronic and Information Technology*, edited by R. Waser (Wiley-VCH, Weinheim, 2003), pp. 527–564.
[2] J. F. Scott, Ferroelectr. Rev. **1**, 1 (1998).
[3] R. Waser, T. Baiatu, and K. H. Hardtl, J. Am. Ceram. Soc. **73**, 1645 (1990); **73**, 1654 (1990); **73**, 1663 (1990).
[4] Y. Sakabe, K. Minai, and K. Wakino, Jpn. J. Appl. Phys. **20**, 147 (1981).
[5] Y. Nakano, A. Sato, A. Hitomi, and T. Nomura, Ceram. Trans. **32**, 119 (1993).
[6] H. Kishi, Y. Mizuno, and H. Chazono, Jpn. J. Appl. Phys., Part 1 **42**, 1 (2003).
[7] Yoed Tsur, Atsushi Hitomi, Ian Scrymgeour, and Clive A. Randall, Jpn. J. Appl. Phys., Part 1 **49**, 255 (2001).
[8] H. Chazono, Y. Inomata, N. Kohzu, and H. Kishi, Key Eng. Mater. **169–170**, 31 (1999).
[9] H. Kishi, Y. Mizuno, and H. Chazono, JSAP Int. **8**, 4 (2003).
[10] Clive A. Randall, J. Ceram. Soc. Jpn. **109**, S2 (2001).
[11] W. Hofman, S. Hoffmann, and R. Waser, Thin Solid Films **305**, 66 (1997).
[12] M. Grossmann, S. Hoffmann, S. Gusowski, R. Waser, S. K. Streiffer, C. Basceri, C. B. Parker, S. E. Lash, and A. I. Kingon, Integr. Ferroelectr. **22**, 83 (1998).
[13] W.-Y. Choi, Y. Tsur, C. A. Randall, and S. Trolier-McKinstry, Mater. Res. Soc. Symp. Proc. **596**, 487 (2000).
[14] R.-V. Wang, P. C. McIntyre, J. D. Baniecki, K. Nomura, T. Shioga, K. Kurihara, and M. Ishii, Appl. Phys. Lett. **87**, 192906 (2005).
[15] J. Ihlefeld, B. Laughlin, A. Hunt-Lowery, W. Borland, A. Kingon, and J-P. Maria, J. Electroceram. **14**, 95 (2005).
[16] O. N. Tufte and P. W. Chapman, Phys. Rev. **155**, 796 (1967).
[17] S. Zafar, B. Hradsky, D. Gentile, P. Chu, R. E. Jones, and S. Gillespie, Appl. Phys. Lett. **86**, 3890 (1999).
[18] S. Saha and S. B. Krupanidhi, J. Appl. Phys. **90**, 1250 (2001).
[19] A. Many and G. Rakavy, Phys. Rev. **26**, 1989 (1962).
[20] R. Meyer, R. Liedtke, and R. Waser, Appl. Phys. Lett. **86**, 112904 (2005).
[21] Rainer Waser, J. Am. Ceram. Soc. **74**, 1934 (1991).
[22] N. H. Chan, R. K. Sharma, and D. M. Smyth, J. Am. Ceram. Soc. **64**, 556 (1981).

Downloaded 19 Jun 2011 to 155.69.4.4. Redistribution subject to AIP license or copyright; see http://apl.aip.org/about/rights_and_permissions